Suyehiro, K., Sacks, I.S., Acton, G.D., and Oda, M. (Eds.)
Proceedings of the Ocean Drilling Program, Scientific Results Volume 186

1. Leg 186 Synthesis: Drilling the Forearc of the Northeast Japan Arc—Causes and Effects of Subduction Plate Coupling over 20 m.y.[1]

I. Selwyn Sacks[2] and Kiyoshi Suyehiro[3]

ABSTRACT

High-recovery core sample and downhole logging data from Sites 1150 (39°11′N, 143°20′E) and 1151 (38°45′N, 143°20′E), drilled during Ocean Drilling Program Leg 186, generally confirmed the Neogene tectonic erosion history as discovered and described by Deep Sea Drilling Project Legs 56, 57, and 87, drilled between 39°44′N and 40°38′N in the northeast Japan Trench forearc. We propose that the sedimentary characteristics of the drilled cores can be explained as consequences of the change in plate coupling between the subducting Pacific plate and the Eurasian plate, dependent on the plate dip angle and water flux resulting from plate subduction. Our model explains the interrelationship among the observed and inferred changes in the plate dip angle, location of the volcanic front, sedimentation rate, volcanic activity, and horizontal stress field caused by the change in plate coupling, which dictates the amount of tectonic force transmitted across the plate boundary. Previously studied subsidence history of the forearc, ascribed to the subduction erosion process, is also incorporated.

INTRODUCTION

During Ocean Drilling Program (ODP) Leg 186, Sites 1150 and 1151, which have contrasting seismic characteristics, were drilled on the deep-sea terrace of the Japan Trench. The main objective of the cruise,

[1]Sacks, I.S., and Suyehiro, K., 2003. Leg 186 synthesis: drilling the forearc of the northeast Japan arc—causes and effects of subduction plate coupling over 20 m.y. *In* Suyehiro, K., Sacks, I.S., Acton, G.D., and Oda, M. (Eds.), *Proc. ODP, Sci. Results,* 186, 1–27 [Online]. Available from World Wide Web: <http://www-odp.tamu.edu/publications/186_SR/VOLUME/SYNTH/SYNTH.PDF>. [Cited YYYY-MM-DD]
[2]Department of Terrestrial Magnetism, Carnegie Institution of Washington, 5241 Broad Branch Road, Northwest, Washington DC 20015-1305, USA. sacks@dtm.ciw.edu
[3]Deep Sea Research Department, Japan Marine Science and Technology Center, 2-15 Natsushima-cho, Yokosuka 237-0061, Japan.

Initial receipt: 2 December 2002
Acceptance: 15 July 2003
Web publication: 5 September 2003
Ms 186SR-119

to establish borehole geophysical observatories at the bottom of these sites (Sacks, Suyehiro, Acton, et al., 2000), was successfully accomplished. Results from these observatories will be published elsewhere (e.g., Araki et al., submitted [N1]). Previous drilling in the area occurred during Deep Sea Drilling Project (DSDP) Legs, 56, 57, and 87, which shed light on subduction erosion tectonics (Scientific Party, 1980; Kagami, Karig, Coulbourn, et al., 1986). New data from Leg 186 cores and downhole logging further confirmed previous findings for the present to the middle Miocene (16.3 Ma), applicable from 38°45′N to 40°38′N. Previous syntheses for sites from this area focused on the forearc history in relation to subduction and volcanism (von Huene et al., 1980, 1982); therefore, we attempt here to present a broad perspective of the Japan forearc-arc-backarc development in terms of plate coupling based on the new results and existing data. Many postcruise biostratigraphic studies provide detailed and precise datum constraints and demonstrate responses to the regional ocean current system (**Maruyama and Shiono; Koizumi and Sakamoto; Li; Hagino and Okada; Kurita and Obuse;** and **Hayashi et al.;** all this volume). Geochemical studies show evidence of the paleoenvironment as well as evidence of fluid flow from depth (**Mora; Ijiri et al.; Fujine et al.;** and **Kopf et al;** all this volume). Sample analyses and the ubiquitous presence of dolomite will provide important constraints to understand the formation and environment of dolomite (**Sakamoto et al.,** this volume).

During the last 20 m.y., the tectonics of the northeast Japan arc system have undergone significant changes. Perhaps the most significant event was the opening of the Japan Sea, which caused the Japan arc to separate from the East Asian continent (e.g., Tamaki et al., 1992). At this time the subduction of the Pacific plate was already ongoing. In the circum-Pacific subduction belt, we observe subduction tectonics of various types (e.g., Jarrard, 1980). It is not yet certain how such variation is manifested. For example, Uyeda and Kanamori (1979) proposed two end-member examples, Chilean type and Mariana type, that occur as a result of a difference in plate coupling. We will address what controls the plate coupling. Any attempts so far to relate various plate subduction parameters to plate coupling and subduction characteristics seem inconclusive (e.g., Uyeda and Kanamori, 1979; Jarrard, 1980; Ruff and Kanamori, 1980). We attempt to detail the subduction history over 20 m.y. using results from drilling in the area (Sacks, Suyehiro, Acton, et al., 2000; von Huene et al., 1980; Kagami, Karig, Coulbourn, et al., 1986) and onland data and to explain the changes using simple models that describe plate coupling (Kincaid and Sacks, 1997; Huang et al., 1998; Wang and Suyehiro, 1999).

We will show that the volcanic front moved much larger distances than the trench axis, requiring a drastic change in the plate dip angle. We can estimate plate coupling based on this change in dip angle, together with the mantle wedge flow model, and explain, at least qualitatively, changes in sedimentation rate, volcanic activity, and extent of the present seismogenic zone.

F1. Cross section across the northeast Japan arc, p. 14.

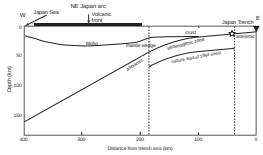

F2. Seismicity and topography of the northeast Japan area, p. 15.

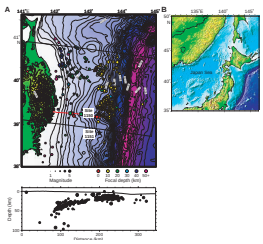

PRESENT SEISMOTECTONIC STATE

In this section, we summarize existing data regarding the seismotectonic state of the northeast Japan arc system, where the Pacific plate is subducting nearly normal to the trench axis at 9–10 cm/yr (Fig. **F1**). Figure **F2** shows recent seismicity in the area. Recent major (M > 7.5) inter-

plate events in this area are the 1968 Tokachi-oki earthquake (Ms = 8.0) (Kanamori, 1971) and 1994 far east off Sanriku earthquake (Ms = 7.5) (Nishimura et al., 1996; Nakayama and Takeo, 1997). The depths of large interplate earthquake rupture zones range from 12 to 55 km (Hasegawa et al., 1994; Suyehiro and Nishizawa, 1994).

Recently, the distribution of microearthquakes in spatial relation to structure in the area has been summarized by Suyehiro and Nishizawa (1994) and Hino et al. (2000). An outstanding feature is the existence of a seismic gap beneath the trench inner slope, the water depth of which is 4–6 km (Hirata et al., 1983, 1985). These microearthquakes occur in clusters, and they have not moved over decades, only changed frequency of activity.

Von Huene et al. (1994) suggested that subducted strata along the plate boundary exists to 12 km depths, thickens beneath the upper and middle slope, and acts as a buffer to control interplate friction. The location of the subducted strata appears to correspond to the low-velocity zone as detected by wide-angle reflection data (Fujie et al., 2002; Takahashi et al., 2000).

For our purpose, it is important to summarize the existing results regarding the transitional change toward the trench axis. The crustal structure of the arc shows a slow Pn velocity of 7.5 km/s and a crustal thickness of 30 km (Yoshii and Asano, 1972). Pn is the upper mantle *P*-wave (V_P) velocity. A more recent model for the Kitakami crustal structure put the Mohorovicic discontinuity (Moho) depth at 32–34 km with Pn velocity >7.7 km/s (Iwasaki et al., 1994). The Moho becomes shallower toward the trench (Zhao et al., 1992). Forearc crustal structures were estimated by many offshore wide-angle refraction surveys (Murauchi and Ludwig, 1980; Nagumo et al., 1980; Suyehiro and Nishizawa, 1994; Takahashi et al., 2000; Ito et al., 2002; Fujie et al., 2002). Suyehiro and Nishizawa (1994) estimated that the subducting angle is 7° at a distance of 110 km from the trench axis and 25° beneath the coastline. Hino et al. (1996) also estimated the subduction angle near the updip limit of the seismogenic zone as ~5°.

Many multichannel seismic (MCS) studies obtained images of the Cretaceous unconformity and subducting strata along the plate boundary (e.g., Nasu et al., 1980; von Huene et al., 1994; Tsuru et al., 2000). Tsuru et al. (2000) imaged deep reflection images of the plate boundary down to ~15 km depth.

Figure **F3** summarizes the outstanding features of these structural models. The tip of the mantle wedge has a significantly higher velocity than beneath the arc and terminates at 20 km depth (Hino et al., 2000; Takahashi et al., 2000; Ito et al., 2002). The lower crust, with V_P > 6.5 km/s, slows to 6.2–6.6 km/s and terminates at a depth range of 12–20 km. We also plotted a zone of high electrical resistivity (Goto et al., 2001) as shown in Figure **F3.**

F3. Seismic velocity and electrical resistivity in the forearc region, p. 16.

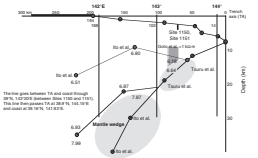

PREVIOUS OCEAN DRILLING RESULTS

Since the DSDP era, five legs had been drilled in the area before ODP Leg 186. They were DSDP Legs 56, 57, and 87, which were drilled in the forearc, and ODP Legs 127 and 128, which were drilled in the backarc of the Japan Sea. Figure **F4** shows the map of the area with drilled holes across northeast Japan.

F4. Map of the forearc region with drilled sites, p. 17.

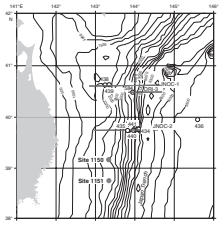

Results of Forearc Drilling

One of the primary results of drilling in the forearc before Leg 186 was the determination of the subsidence history of the forearc over ~20 m.y. and the discovery of a subduction erosion regime (von Huene et al., 1982), which is now considered an important process of plate subduction. A summary of the forearc drilling results according to von Huene et al. (1982) is (1) there were periods of explosive volcanism separated by a long Paleogene interval without volcanism; (2) massive Neogene subsidence of the forearc area occurred simultaneously with arc volcanism; and (3) in the Pliocene, steepening of the landward slope of the trench changed the slope basins from areas of rapid sediment accumulation to areas of erosion. Another surprise was the unexpected discovery of andesitic volcanic rocks at Site 439, 90 km inward of the trench axis, which indicated that there is an offset of ~200 km between the present arc and where Oligocene volcanism occurred.

The advancement of coring technology allowed us to increase the deep core recovery rate from <50% to ~70%. Using advanced piston coring, less disturbed sediment cores were recovered at nearly full recovery. We summarize here various results of Leg 186 that we intend to explain in terms of the tectonic history of the island arc system.

Volcanism

Figure F5 is a plot of ash records from Sites 1150 and 1151 as well as Leg 56 and 57 sites. It is apparent that there was a major increase in volcanic deposits at Site 1150 at ~3 Ma and a decrease in the most recent ~0.5 m.y. At Site 1151, the increase starts at ~4 Ma. Farther north (40.6°N), in Hole 438A, volcanism increased from ~5 until ~2 Ma.

F5. Ash patches indicating volcanic activity, p. 18.

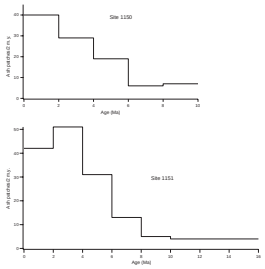

Sedimentation Rate

Sedimentation rates at Sites 1150 and 1151 are given and plotted in Figure F6 after corrections for compaction, which are insignificant but are nonetheless incorporated. The overall feature is a relative low between 16 and 10–8 Ma, an increase to peak rates at 6–4 Ma, then a decrease to 3–2 Ma. This change of trend occurred as the stress field changed from tensional to compressional or from arc subsidence to uplift. If we compare the trend with Figure F5, the overall pattern is similar. The time difference of the peaks may be partly due to age uncertainties, though some could be real.

F6. Sedimentation rates, p. 19.

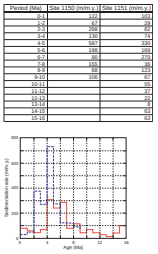

Geochemistry

Chemical analyses of pore waters show that chlorinity gradually decreases with depth from ~550 mM at the top of Site 1150 to 500 mM at ~200 meters below seafloor (mbsf). From ~550 mbsf, values abruptly decrease with depth to reach a minimum of 350 mM at ~700 mbsf. Chlorinity at Site 1151 also decreases with depth, with somewhat different characteristics, but the magnitude of change is similar to that at Site 1150 (Fig. F7). A similar trend is observed in the magnesium, potassium, and alkalinity profiles at both sites. Kopf et al. (this volume) summarized that the profound excursion in gas and water profiles can be best explained by deep-seated processes. We will refer to these results as supporting evidence of water flux, which influences the mechanical plate coupling.

F7. Chlorinity of interstitial water, p. 20.

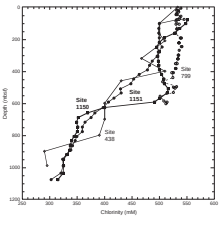

Results of Backarc Drilling

Japan Sea drilling has provided ages of basement basalts that range from 24 to 17 Ma (Tamaki, Suyehiro, Allan, McWilliams, et al., 1992). Together with stratigraphic constraints of subsidence history (Ingle, 1992) and marine geomagnetic data, Tamaki et al. (1992) proposed the evolution scenario of the backarc area to be in extension from 32 to 10 Ma, during which time the Japan Sea opened and formed between 28 and 18 Ma. The initiation of widespread uplift and the compressional regime occurred between 10 and 7 Ma, which accelerated at ~5 Ma and experienced extremely high rates of uplift (~500 m/m.y.) between 2 and 0 Ma.

Jolivet and Tamaki (1992) related volcanic events and tectonic phases. In particular, they pointed out the starvation of the volcanic activity between 10 and 7 Ma coincided with the stress field change presented above. The variation of ash layers with time (14–4 Ma) was found to be similar to the data from the forearc, suggesting the eruption source to be the Japan arc.

Onland Geology

We follow Sato and Amano (1991), who summarized the geological history of the northeast Japan arc since ~22 Ma mainly based on onland stratigraphy across the arc between 38° and 39°N. They proposed to recognize four temporal stages in the development of the arc. The first is the rifting stage (~22–15 Ma), characterized by formation of the half-grabens, extensional tectonics, volcanism, and high rates of sedimentation, which coincided with the opening of the Japan Sea. The second is the backarc basin opening stage (15–13 Ma), during which time the backarc side subsided rapidly. Then the transitional stage (13–2.4 Ma) followed with a thermal subsidence substage (13–8 Ma) and transition to compressional substage (8–2.4 Ma). The fourth is the shortening deformation stage (2.4 Ma to present), when the stress field became compressional (Fig. F8).

F8. Stress field change since 22 Ma, p. 21.

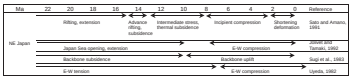

Mechanical Coupling between the Subducting Slab and the Overlying Plate

Uyeda and Kanamori (1979) classified the subduction zones into two end-member types, namely Chilean and Mariana types. The former is strongly coupled and characterized by truly large earthquakes, shallow-dipping subduction slab, and no active backarc spreading. Uyeda (1982) reviewed the case of the northeast Japan arc and suggested that the arc changed from Mariana- to Chilean-type mode based on the subsidence history of the inner trench slope, which showed a shift from subsidence to uplift in the Pliocene. He suggested the depth change, if it represents the shallowing of the depth of the trench, may indicate the mode change. He also refers to supportive lines of evidence to recent stress change from tensional (21–7 Ma) to compressional in the direction of subduction (Nakamura and Uyeda, 1980) and to vertical movement change from subsidence (17–10 Ma) to uplift in the Quarternary (Sugi et al., 1983).

A simple model of plate interaction was proposed to explain contrasting subduction stress systems between northeast Japan and southwest Japan (Wang and Suyehiro, 1999). The northeast Japan stress field is basically east-west compressional over a wide area, whereas that of

southwest Japan is arc-parallel compression. Such a feature can be explained by the difference in the dip angle and the length of the stress transfer zone, keeping other parameters the same. This model is supported by observations of the intraplate earthquake mechanisms and the length of the zone of interplate thrust earthquakes, which are proxies of the stress field and the plate locked zone. A locked zone may be considered a shear stress transfer zone.

Volcanic Front and Subduction Angle

Jarrard (1980) compiled subduction parameters around the globe and showed that the distance between the trench and arc is highly correlated (R = 0.91) to the plate dip angle. He obtained

$$\text{Gap} = 51 + 81.4/\tan(\text{DipI}),$$

where,

gap = the horizontal distance between the trench axis and the arc.
DipI = the intermediate dip angle down to 100 km depth.

These subduction zones include arc ages of 6–226 Ma; age is only weakly correlated with gap distance (R = 0.44). On the same Pacific plate today, the dip beneath the Marianas is steep, whereas beneath Tohoku it is shallow. Therefore, global observation indicates that the present arc position is more strongly dependent on the present dip angle than on age. More importantly, the depth to slab from the arc can be roughly obtained by multiplying gap and tan(DipI), which results in ~103 ± 13 km (neglecting the Philippine plate because the present slab has not reached the arc). Indeed, it has been commonly observed that at present the depth of the slab beneath the volcanic front is generally ~100 km over a large range of slab dips. We assume that was the case in the Neogene also. The depth of magma segregation has been constant since 20 Ma (Tatsumi et al., 1994). This suggests that if we can reconstruct the arc history, the subduction dip angle history can also be estimated.

According to the geologic history described above, the location of the volcanic front (VF) changed with time (Ohguchi et al., 1989; Sato, 1994). Figure **F9** shows the migration of the volcanic front from Ohguchi et al. (1989). The VF existed at the eastern margin of the present Japan Sea at 30 Ma and moved to the Kitakami area and off Fukushima between 25 and 22 Ma. Then the VF moved to its present position at ~12 Ma. Ohguchi et al. (1989) suggest steepening of the subduction angle from the migration of the volcanic front (Ohguchi et al., 1989). Pollitz (1986) suggested the shift to compressional state may be related to the absolute motion change of the Pacific plate between 5.2 and 2.5 Ma (Pollitz, 1986).

Figure **F10** shows the change in plate geometry over time required by the position of the VF and the fixed depth to the subducting slab. The effect of subduction erosion causing the trench axis to move inward is small compared with the overall geometry change. We will now proceed to show that these inferred changes in plate dip angle can explain the change in the stress field inferred from geological records. In order to do so, we need to refer to temperature-controlled behavior of the crust and mantle and surface effects of mechanical coupling.

F9. Migration of the volcanic front, p. 22.

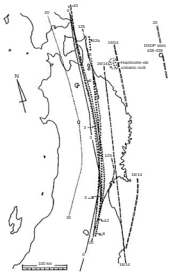

F10. Change in plate geometry over time, p. 23.

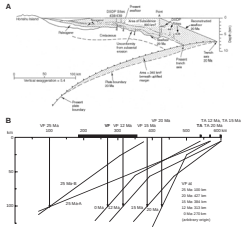

EFFECTS OF THERMAL STRUCTURE AND MANTLE WEDGE FLOW

The mechanical behavior of the crust and upper mantle materials is temperature controlled; therefore, we first examine the geometry effects on the thermal structure.

Two competing factors affect the thermal evolution of subduction zones. The subducting slab cools its environment, but the forced return flow brings in hot material. Kincaid and Sacks (1997) conducted numerical convection experiments in a viscous, Boussinesq, Newtonian fluid within a two-dimensional Cartesian geometry. Fluid motion was due both to thermal convection and slab penetration. Slab geometry was not specified; it was found to be sensitive to slab buoyancy and slab velocity.

For parameters appropriate to northeast Japan subduction, a rather similar linear slab was found. The time-dependent evolution was examined for a wide range of parameter space. We rely on some conclusions that were found to be quite robust. For a relatively shallow slab dip angle such as is appropriate to present-day northeast Japan, cooling by the slab dominates. For steeply dipping slabs such as the Marianas, the hot return flow controls the temperature.

Importantly for our study, the shallow dip case leads to a runaway process, which dominates the mechanical interaction of the subducting plate and the overlying structure. Because at this geometry the cooling of mantle material near the apex of the mantle wedge both to the overlying crust and to the slab overwhelms the heating by the return flow, the material viscosity increases and it tends to be more sluggish. This gives it more time to cool, and so its viscosity continues to increase until it becomes almost static. Eventually, this frozen "nose" extends from the apex and nearly reaches the volcanic front. The time required to reach this condition is estimated to be on the order of 3 m.y. Figure **F11** shows the nose growth as a function of time. The effect of this now rigid wedge is to increase the coupled length between the slab and the overlying plate.

F11. Development of stiffened mantle wedge, p. 24.

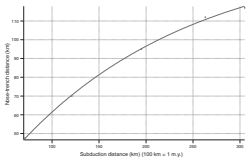

Honda (1985) also constructed a model of thermal structure of the northeast Japan area to fit the heat flow observation using available geophysical, geochemical, and geological constraints. His modeling required the existence of a rigid (nonmoving) mantle nose region with low temperature bounded by the subducting slab extending about halfway to the VF from the trench. This portion corresponds to the high-velocity mantle area (V_P = 8.0 km/s) (Fig. **F3**).

Mechanical Coupling and Erosion Rate

Mechanical coupling affects mountain growth and continental deformation. Huang et al. (1998) examined the deformation of northeast Japan resulting from long-term (5 m.y.) interaction with the Pacific slab. A finite element model, TECTON, from Melosh and Raefsky (1980) and Wallace and Melosh (1994) was modified to include dynamically applied fracture criteria and erosion and deposition. Because the strike of folds and faults in northeast Japan are approximately normal to the direction of subduction, a two-dimensional plane-strain analysis is adequate. The strength profile of the lithosphere was based on experimentally determined rheology laws (Wilks and Carter, 1990) and

temperature derived from heat flow data (Furukawa and Uyeda, 1989). The criteria for a successful model are that the topography, gravity residual anomaly, and seismicity must match the observations.

The output of the model is the coupling force between the subducting slab and the overlying continent and its depth distribution. Additionally, the erosion and sedimentation rates are determined. The huge gravity residual anomaly of +75 mGal over the Kitakami range is supported by the warp generated by the strong coupling of the Pacific plate down to ~50 km. This is consistent with the observation of thrust earthquakes on the interface down to this depth (e.g., Hasegawa et al., 1994). The mantle wedge must be rigid enough to not only store strain released by earthquakes but also to provide long-term support for the warps.

The growth rate of the near coastal range, the Kitakami, as well as the Backbone range is proportional to the compressional force applied by the subducting Pacific plate. Ohmori (1978) showed that the erosion rate is proportional to the square of the elevation, and his estimated value of 0.3 mm/yr for a height of 1000 m was used in the model runs (Huang et al., 1998). Whereas erosion is readily calculated, deposition of the erosion products is more complicated. Downwarps on land get filled, but we assume much of the sedimentation can be represented by offshore depositions.

Relating Coupling to Geometry

The results from the two models described above can be used to relate the proposed changes in the subduction geometry to observables such as sedimentation rate and volcanic flux determined from the ODP and DSDP holes in the forearc (Figs. **F6, F7**).

The proposed model geometry showing plate-coupled zone length spanning 20 m.y. is shown in Figure **F12.** At 20 Ma the slab geometry is very similar to that of present-day Marianas. The distance of the postulated volcano identified in Hole 439 to the trench is similar to that in the Marianas arc. Backarc spreading occurs in this arc, and by analogy with Japan at ~20 Ma, tension in Japan and opening of the Japan Sea would be expected.

By 14 Ma the volcanic front reached the Japanese island, shown in Figure **F9.** As well as the dip change, there also had to be tectonic erosion of the overlying crust starting at least at 20 Ma. This erosion was continuous, as the graben formed by the bending of the Pacific plate could scrape material off the bottom of the overlying plate. This caused the slab and, therefore, the volcanic front to advance by ~30 km/10 m.y. (von Huene et al., 1994). In addition, at this stage the slab may not have been at its equilibrium shallow dip yet. This also caused westward migration (Fig. **F10**). The shallow dip angle encouraged cooling and eventual freezing out of the mantle wedge. By 6 Ma this stiff zone reached its maximum (equilibrium) extent and the mechanical interaction between the subducted slab and the overlying material was also at a maximum.

Coupling Length and Water Flux

We have so far only discussed the thermal effects of the subducted cool slab on the temperature-dependent viscosity of the overlying mantle. In addition, water is released from the slab. Ultimately, some of this water flux induces melting in the mantle and causes volcanism. Recent

F12. Estimated plate coupling length change since 20 Ma, p. 25.

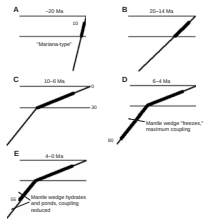

measurements of boron isotopes suggest that the slab releases ^{11}B-enriched fluids from the shallowest levels to depths below 200 km (Benton et al., 2001). If this water is released into material with a temperature below its wet solidus, hydrous phases will form. Eventually, the static mantle wedge will become hydrated. This causes lower seismic velocities (Fig. F3) and intermediate resistivity. Later, the vicinity of the slab interface will become saturated and further water release will give rise to high pore pressure and, finally, free water. Since this is a cumulative process downslab, the excess will first appear at the greatest depth (i.e., the deepest part of the static wedge).

The effect of the high pore pressure is to reduce the mechanical coupling (shear) between the slab and the overlying static mantle. This reduced coupling length has a strong effect on the eastern mountain building. As shown in Huang et al. (1998), the Kitakami range requires the force couple provided by the deeper locked zone. Reduction of the coupling length affects the mountain building and therefore the erosion, which is the only observation, in two ways; both the coupling torque and the coupling length are reduced.

Coupling Length Model

In order to model the effect of the coupled length on the resultant force, we follow the reasoning of Wang and Suyehiro (1999). Making the simplest assumption that friction was constant, it follows that the force on the overlying plate would be simply proportional to the coupled length. The coupling lengths are shown schematically in Figure F12. The slab contact length in the crust depends on erosion, as is shown in Figure F10.

Using water depth as a determinant, erosion has been modeled by Lallemand et al. (1992) and von Huene and Lallemand (1990). Since the water depth is affected not only by the erosion but also by the sediment load and the slab coupling, the calculation is complex. For the purpose of this model, we assume a simple progression because we only require a plausible rate. We applied the modeling techniques described above to the slab geometry changes postulated from the volcanic arc position shown in Figure F10. The primary data that we had to match were the sedimentation rate and volcanic flux (ash) data determined from the cores taken during ODP Leg 186. Figure F6 shows the parameters of the calculation. The results are shown in Figure F13. Although it is not possible to determine the deposition paths well enough to quantify the sedimentation offshore, we can calculate the profile of the temporal changes in sedimentation rate.

The effect of water saturation leading to high pore pressures will not only reduce the coupling length and limit the seismic thrust zone depth (to ~55 km) but will also affect the volcanic flux. The wedge had cooled sufficiently to become essentially static and to couple strongly by ~6 Ma, though the coupling may have started increasing from ~10 Ma (Figs. F10, F12). The overlying mantle became increasingly hydrated and less absorbent until ~4 Ma, when high pore pressure and free water existed below the seismic thrust zone. The free water traveled with the slab until it reached hot, mobile mantle with a temperature at least above its wet solidus; there it will flux melt. This water added to that which comes from dehydration of slab minerals such as amphibole, so the volcanic flux increased. Note that the model prediction is that the increase in volcanic flux should occur when the sedimentation rate decreases, as is observed.

F13. Relation of sedimentation rate and volcanic flux to age, p. 26.

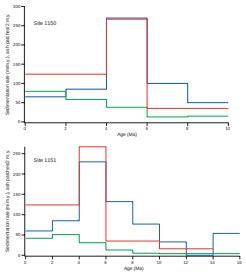

SUMMARY

Our model highlights the importance of the subduction angle on the tectonic mode and volcanism. The reason for the sensitivity is that for steep (Mariana type) subduction mantle return flow maintains a hot wedge, whereas for flatter subduction (Tohoku type) the mantle return flow is sufficiently cooled by the slab and through the overlying crust that it stiffens and eventually becomes static. The stress environment becomes increasingly compressive as the wedge stiffens and the mechanical coupling length between the slab and the overlying plate lengthens. This enhanced compressive stress accelerates mountain building, which in turn causes faster erosion. The sedimentation due to this erosion is one of our principal observables.

As water is continuously released from the slab into the increasingly static overlying mantle, this region hydrates and eventually saturates. Further water release causes overpressured zones. The condition can be observed in the cores by two effects: the strong mechanical coupling length is reduced, resulting in reduced sedimentation, and the water, previously absorbed in the overlying wedge, is transferred to the volcanic front, causing increased volcanism. Note that mature Tohoku-type subduction geometry is the only type that should cause a voluminous volcanic front such as that observed in the Quaternary. It will not occur with the transitional or earlier geometry, as is also observed.

We have shown that this model is consistent with many different types of data and that it provides a framework so that it can be tested by other data in the future.

ACKNOWLEDGMENTS

This research used samples and data provided by the Ocean Drilling Program (ODP). The ODP is sponsored by the U.S. National Science Foundation (NSF) and participating countries under management of Joint Oceanographic Institutions (JOI), Inc. Funding for this research was provided by ODP. Discussions with Roland von Huene were very helpful.

REFERENCES

Benton, L.D., Ryan, J.G., and Tera, F., 2001. Boron isotope systematics of slab fluids as inferred from a serpentine seamount, Mariana forearc. *Earth Planet. Sci. Lett.*, 187:273–282.

Fujie, G., Kasahara, J., Hino, R., Sato, T., Shinohara, M., and Suyehiro, K., 2002. A significant relation between seismic activities and reflection intensities in the Japan Trench region. *Geophys. Res. Lett.*, 29:10.1029/2001GL013764.

Furukawa, Y., and Uyeda, S., 1989. Thermal state under the Tohoku arc with consideration of crustal heat generation. *Tectonophys.,* 164:175–187.

Goto, T., Mikada, H., Fujie, G., Suyehiro, K., Kaneda, Y., Tsuru, T., Uhira, K., Kodaira, S., Nakanishi, A., Sayanagi, K., Uyeshima, M., Utada, H., Seama, N., and Constable, S., 2001. Electromagnetic survey across the northern Japan Trench, off-Sanriku, Japan. *Jpn. Earth Planet. Sci. Joint Mtg.,* S2-P012. (Abstract)

Hasegawa, A., Horiuchi, S., and Umino, N., 1994. Seismic structure of the northeastern Japan convergent margin: a synthesis. *J. Geophys. Res.,* 99:22295–22311.

Hino, R., Ito, S., Shiobara, H., Shimamura, H., Sato, T., Kanazawa, T., Kasahara, J., and Hasegawa, A., 2000. Aftershock distribution of the 1944 Sanriku-oki earthquake (M_W 7.7) revealed by ocean bottom seismographic observation. *J. Geophys. Res.,* 105:21697–21710.

Hino, R., Kanazawa, T., and Hasegawa, A., 1996. Interplate seismic activity near the northern Japan Trench deduced from ocean bottom and land-based seismic observations. *Phys. Earth Planet. Inter.,* 93:37–52.

Hirata, N., Kanazawa, T., Suyehiro, K., and Shimamura, H., 1985. A seismicity gap beneath the inner wall of the Japan Trench as derived by ocean bottom seismograph measurement. *Tectonophys.,* 112:193–209.

Hirata, N., Yamada, T., Shimamura, H., Inatani, H., and Suyehiro, K., 1983. Spatial distribution of microearthquakes beneath the Japan Trench from ocean bottom seismographic observations. *Geophys. J. R. Astron. Soc.,* 73:653–669.

Honda, S., 1985. Thermal structure beneath Tohoku, northeast Japan—a case study for understanding the detailed thermal structure of the subduction zone. *Tectonophys.,* 112:69–102.

Huang, S., Sacks, I.S., and Snoke, J.A., 1998. Compressional deformation of island-arc lithosphere in northeastern Japan resulting from long-term subduction-related tectonic forces: finite-element modeling. *Tectonophys.,* 287:43–58.

Ingle, J.C., Jr., 1992. Subsidence of the Japan Sea: stratigraphic evidence from ODP sites and onshore sections. *In* Tamaki, K., Suyehiro, K., Allan, J., McWilliams, M., et al., *Proc. ODP, Sci. Results,* 127/128 (Pt. 2): College Station, TX (Ocean Drilling Program), 1197–1218.

Ito, A., Hino, R., Nishino, M., Fujimoto, H., Miura, S., Kodaira, S., and Hasemi, A., 2002. Deep crustal structure of the northeastern Japan forearc by a seismic exploration using an airgun-array. *Jishin,* 54:507–520.

Iwasaki, T., Yoshii, T., Moriya, T., Kobayashi, A., Nishiwaki, M., Tsutsui, T., Iidaka, T., Ikami, A., and Matsuda, T., 1994. Precise *P* and *S* wave velocity structures in the Kitakami massif, northern Honshu, Japan, from a seismic refraction experiment. *J. Geophys. Res.,* 99:22187–22204.

Jarrard, R.D., 1980. Relations among subduction parameters. *Rev. Geophys.,* 25:217–284.

Jolivet, L., and Tamaki, K., 1992. Neogene kinematics in the Japan Sea region and volcanic activity of the northeast Japan arc. *In* Tamaki, K., Suyehiro, K., Allan, J., McWilliams, M., et al., *Proc. ODP, Sci. Results,* 127/128 (Pt. 2): College Station, TX (Ocean Drilling Program), 1311–1331.

Kagami, H., Karig, D.E., Coulbourn, W.T., et al., 1986. *Init. Repts. DSDP,* 87: Washington (U.S. Govt. Printing Office).

Kanamori, H., 1971. Focal mechanism of the Tokachi-oki earthquake of May 16, 1968: contortion of the lithosphere at a junction of two trenches. *Tectonophys.,* 12:1–13.

Kincaid, C., and Sacks, S., 1997. Thermal and dynamical evolution of the upper mantle in subduction zones. *J. Geophys. Res.,* 102:12295–12315.

Lallemand, S., Schnurle, P., and Manoussis, S., 1992. Reconstruction of subduction zone paleogeometries and quantification of upper plate material losses caused by tectonic erosion. *J. Geophys. Res.,* 97:217–239.

Melosh, H.J., and Rafesky, A., 1980. The dynamical origin of subduction zone topography. *Geophys. J. R. Astron. Soc.,* 60:333–354.

Moore, G.W., and Fujioka, K., 1980. Age and origin of dacite boulder conglomerate anomalously near the Japan Trench. *In* Scientific Party, *Init. Repts. DSDP,* 56, 57 (Pt. 2): Washington (U.S. Govt. Printing Office), 1083–1088.

Murauchi, S., and Ludwig, W.J., 1980. Crustal structure of the Japan Trench: the effect of subduction of ocean crust. *In* Scientific Party, *Init. Repts. DSDP,* 56, 57 (Pt. 1): Washington (U.S. Govt. Printing Office), 463–469.

Nagumo, S., Kasahara, J., and Koresawa, S., 1980. OBS airgun seismic refraction survey near Sites 441 and 434 (J-1A), 438 and 439 (J-12), and proposed Site J-2B: Legs 56 and 57, Deep Sea Drilling Project. *In* Scientific Party, *Init. Repts. DSDP,* 56, 57 (Pt. 1): Washington (U.S. Govt. Printing Office), 459–462.

Nakamura, K., and Uyeda, S., 1980. Stress gradient in arc-back arc regions and plate subduction. *J. Geophys. Res.,* 85:6419–6428.

Nakayama, W., and Takeo, M., 1997. Slip history of the 1994 Sanriku-Haruka-Oki, Japan, earthquake deduced from strong-motion data. *Bull. Seismol. Soc. Am.,* 87:918–931.

Nasu, N., von Huene, R., Ishiwada, Y., Langseth, M., Bruns, T., and Honza, E., 1980. Interpretation of multichannel seismic reflection data, Legs 56 and 57, Japan Trench transect, Deep Sea Drilling Project. *In* Scientific Party, *Init. Repts. DSDP,* 56, 57 (Part 1): Washington (U.S. Govt. Printing Office), 489–503.

Nishimura, T., Nakahara, H., Sato, H., and Ohtake, M., 1996. Source process of the 1994 far east off Sanriku earthquake, Japan, as inferred from a broad-band seismogram. *Tohoku Geophys. J.,* 34:121–134.

Ohguchi, T., Yoshida, T., and Okami, K., 1989. Historical change of the Neogene and Quaternary volcanic field in the northeast Honshu arc, Japan. *Chishitsugaku Ronshu* [*Geol. Soc. Jpn. Mem.*], 32:431–455.

Ohmori, H., 1978. Relief structure of the Japanese mountains and their stages in geomorphic development. *Bull. Dep. Geogr., Univ. Tokyo,* 10:31–85.

Pollitz, F.F., 1986. Pliocene change in Pacific-plate motion. *Nature,* 320:738–741.

Ruff, L., and Kanamori, H., 1980. Seismicity and the subduction process. *Phys. Earth Planet. Inter.,* 23:240–252.

Sacks, I.S., Suyehiro, K., Acton, G.D., et al., 2000. *Proc. ODP, Init. Repts.,* 186 [CD-ROM]. Available from: Ocean Drilling Program, Texas A&M University, College Station TX 77845-9547, USA.

Sato, H., 1994. The relationship between late Cenozoic tectonic events and stress field and basin development in northeast Japan. *J. Geophys. Res.,* 99:22261–22274.

Sato, H., and Amano, K., 1991. Relationship between tectonics, volcanism, sedimentation and basin development, Late Cenozoic, central part of northern Honshu, Japan. *Sediment. Geol.,* 74:323–343.

Scientific Party, 1980. *Init. Repts. DSDP,* 56, 57: Washington (U. S. Govt. Printing Office).

Sugi, N., Chinzei, K., and Uyeda, S., 1983. Vertical crustal movements of north-east Japan since middle Miocene. *In* Hilde, T.W., and Uyeda, S. (Eds.), *Geodynamics of the Western Pacific-Indonesian Region.* Am. Geophys. Union, Geodyn. Ser., 1:317–330.

Suyehiro, K., and Nishizawa, A., 1994. Crustal structure and seismicity beneath the forearc off northeastern Japan. *J. Geophys. Res.,* 99:22331–22348.

Takahashi, N., Kodaira, S., Tsuru, T., Park, J.-O., Kaneda, Y., Kinoshita, H., Abe, S., Nishino, M., and Hino, R., 2000. Detailed plate boundary structure off northeast Japan coast. *Geophys. Res. Lett.,* 27:1977–1980.

Tamaki, K., Suyehiro, K., Allan, J., Ingle, J.C., Jr., and Pisciotto, K.A., 1992. Tectonic synthesis and implications of Japan Sea ODP drilling. *In* Tamaki, K., Suyehiro, K., Allan, J., McWilliams, M., et al., *Proc. ODP, Sci. Results,* 127/128 (Pt. 2): College Station, TX (Ocean Drilling Program), 1333–1348.

Tamaki, K., Suyehiro, K., Allan, J., McWilliams, M., et al., 1992. *Proc. ODP, Sci. Results,* 127/128 (Pt. 2): College Station, TX (Ocean Drilling Program).

Tatsumi, Y., Furukawa, Y., and Yamashita, S., 1994. Thermal and geochemical evolution of the mantle wedge in the northeast Japan arc, 1. Contribution from experimental petrology. *J. Geophys. Res.: B,* 99:22275–22283.

Tsuru, T., Park, J.-O., Takahashi, N., Kodaira, S., Kido, Y., Kaneda, Y., and Kono, T., 2000. Tectonic features of the Japan Trench convergent margin and fracture zones beneath northeastern Japan revealed by multi-channel seismic reflection data. *J. Geophys. Res.,* 105:16403–16413.

Uyeda, S., 1982. Subduction zones: an introduction to comparative subductology. *Tectonophys.,* 81:133–159.

Uyeda, S., and Kanamori, H., 1979. Back-arc opening and the mode of subduction. *J. Geophys. Res.,* 84:1049–1061.

von Huene, R., Klaeschen, D., Cropp, B., and Miller, J., 1994. Tectonic structure across the accretionary and erosional parts of the Japan Trench margin. *J. Geophys. Res.,* 99:22349–22361.

von Huene, R., and Lallemand, S., 1990. Tectonic erosion along the Japan and Peru convergent margins. *Geol. Soc. Am. Bull.,* 102:704–720.

von Huene, R., Langseth, M., Nasu, N., and Okada, H., 1980. Summary, Japan Trench transect. *In* Scientific Party, *Init. Repts. DSDP,* 56, 57 (Part 1): Washington (U.S. Govt. Printing Office), 473–488.

————, 1982. A summary of Cenozoic tectonic history along IPOD Japan Trench transect. *Geol. Soc. Am. Bull.,* 93:829–846.

Wallace, M.H., and Melosh, H.J., 1994. Buckling of a pervasively faulted lithosphere. *Pure Appl. Geophys.,* 142:239–261.

Wang, K., and Suyehiro, K., 1999. How does plate coupling affect crustal stresses in northeast and southwest Japan? *Geophys. Res. Lett.,* 26:2307–2310.

Wilks, K.R., and Carter, N.L., 1990. Rheology of some continental lower crustal rocks, *Tectonophys.,* 182:57–77.

Yoshii, T., and Asano, S., 1972. Time-term analyses of explosion seismic data. *J. Phys. Earth,* 20:47–57.

Zhao, D., Hasegawa, A., and Horiuchi, S., 1992. Tomographic imaging of *P* and *S* wave velocity structure beneath northeastern Japan. *J. Geophys. Res.,* 97:19909–19928.

Figure F1. Schematic view of the cross section across the northeast Japan arc. Old (>120 Ma) Pacific plate is subducting nearly normal to the trench axis at 9–10 cm/yr. The top plate boundary reaches a depth of ~50 km beneath the eastern coastline. The volcanic front (VF) is ~100 km above the plate boundary. The Japan Sea is a backarc marginal sea. The horizontal stress field is east-west compression at present. The 1994 event ruptured from the shallow end to the deep end of the seismogenic zone.

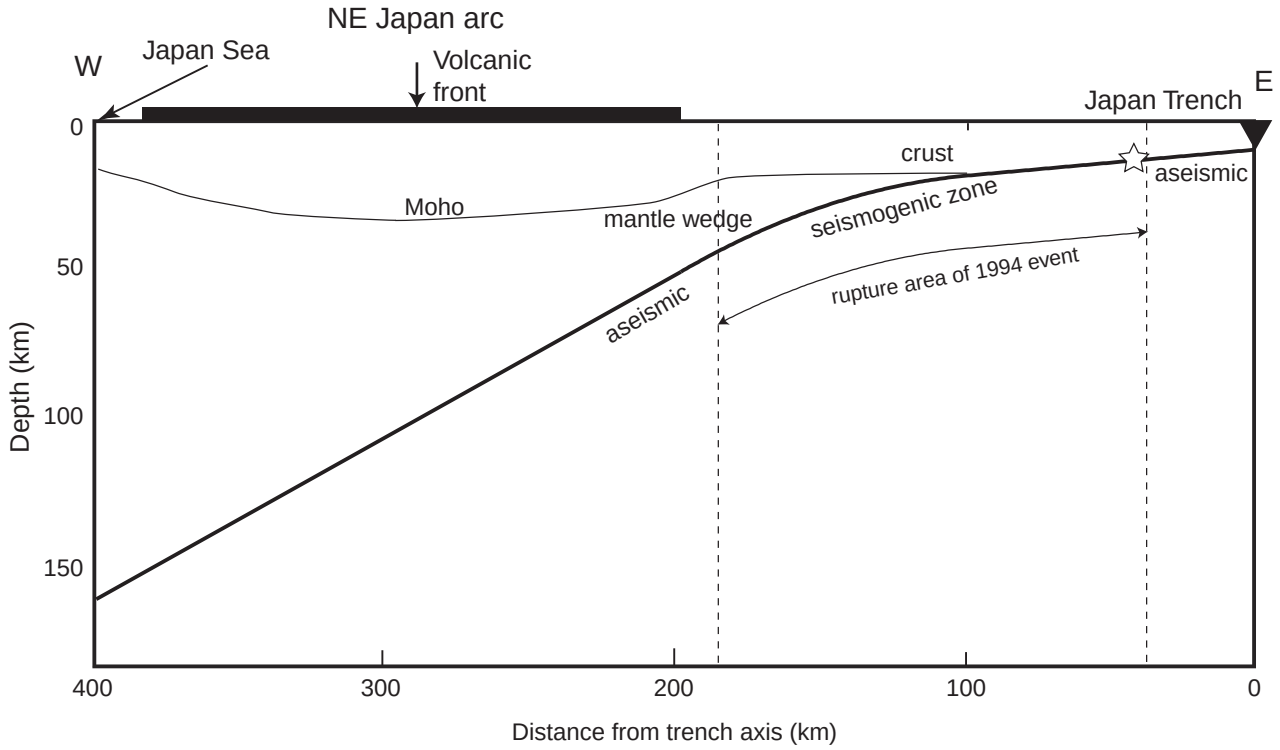

Figure F2. A. Seismicity defining past large thrust earthquake rupture zones. **B.** Topography of the northeast Japan area.

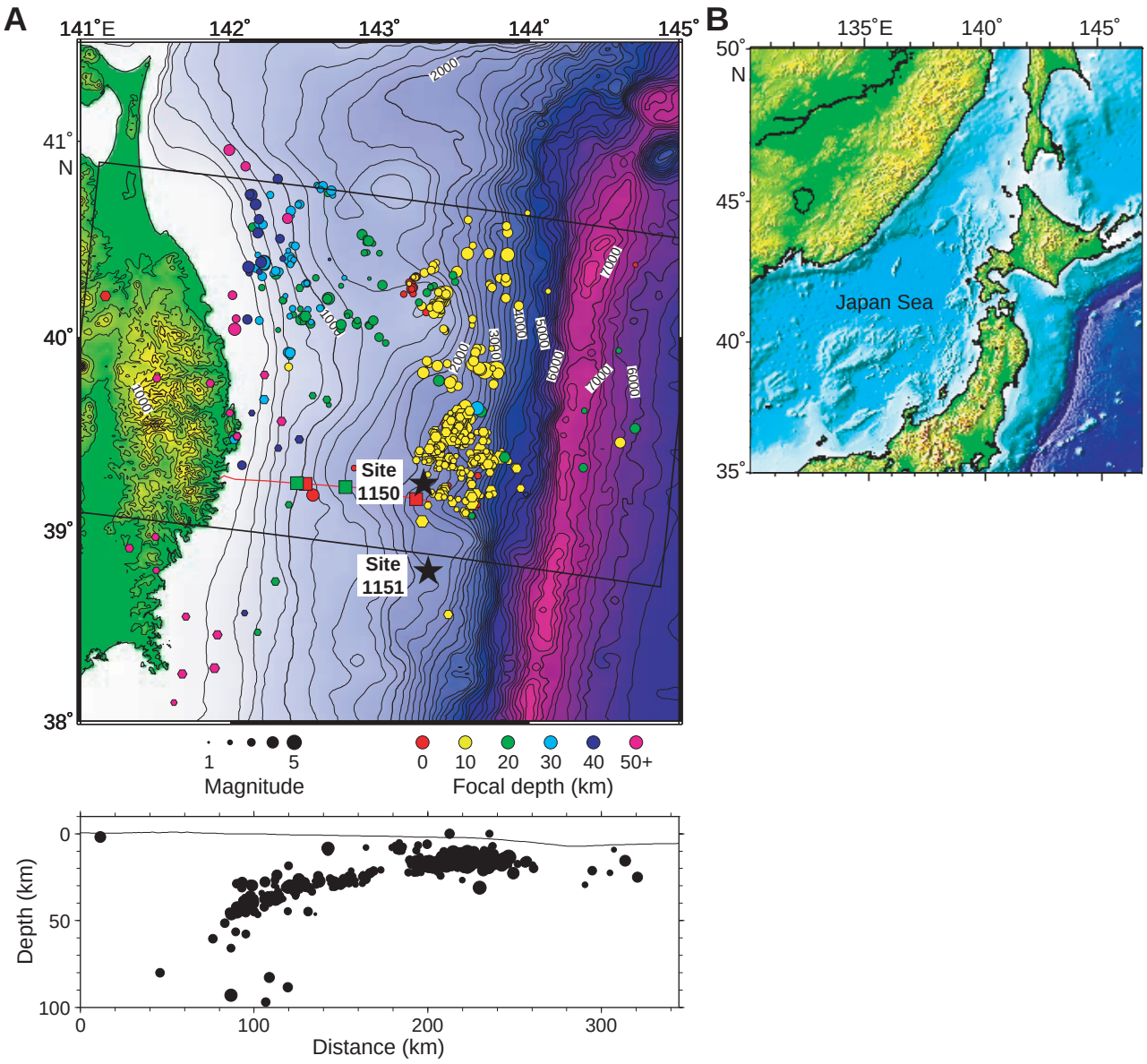

Figure F3. Seismic velocity and electrical resistivity structure in the forearc region (from Suyehiro and Nishizawa, 1994; Hino et al., 2000; Tsuru et al., 2000; Ito et al., 2002; Goto et al., 2001). Shaded areas are seismically active parts of the interplate boundary proximity (Suyehiro and Nishizawa, 1994; Hino et al., 1996).

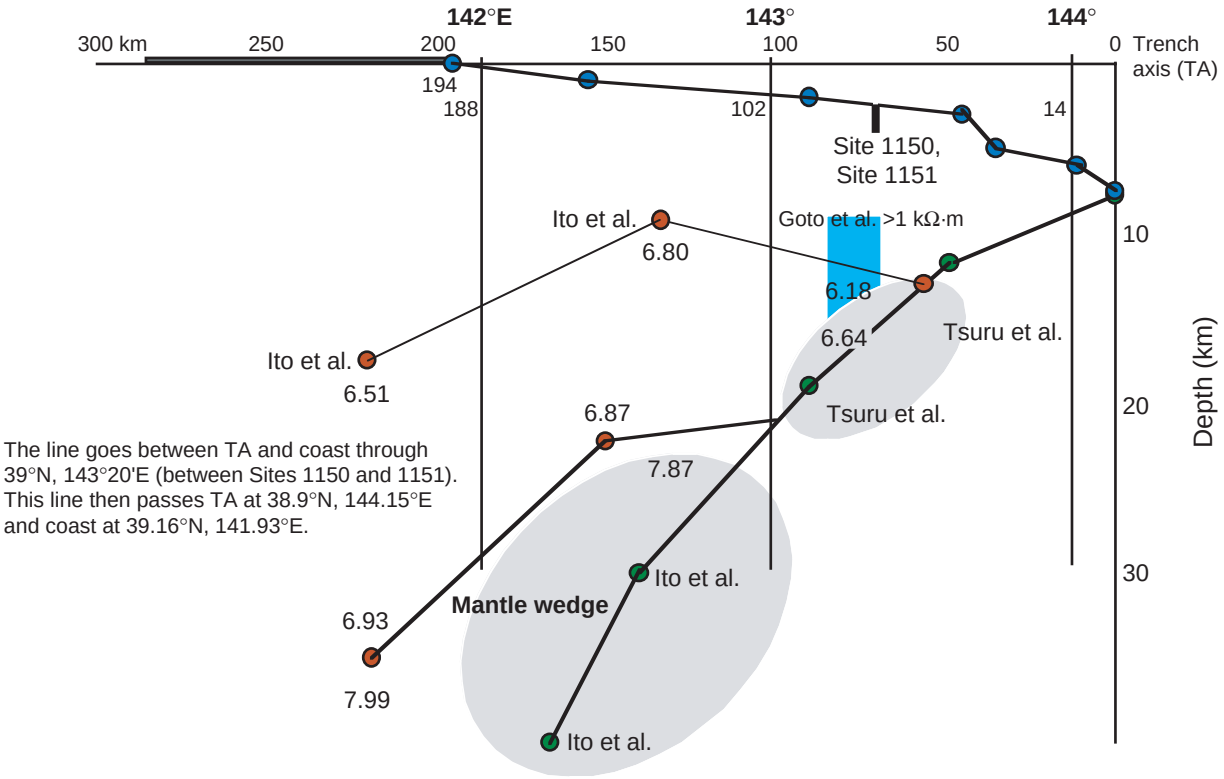

Figure F4. Map of the forearc region with drilled sites. DSDP Leg 56 Sites 434–436; Leg 57 Sites 438, 440, and 441; and Leg 87 Site 548 and ODP Leg 186 Sites 1150 and 1151. Site 1150 is in a seismically active zone and Site 1151 is in an aseismic zone.

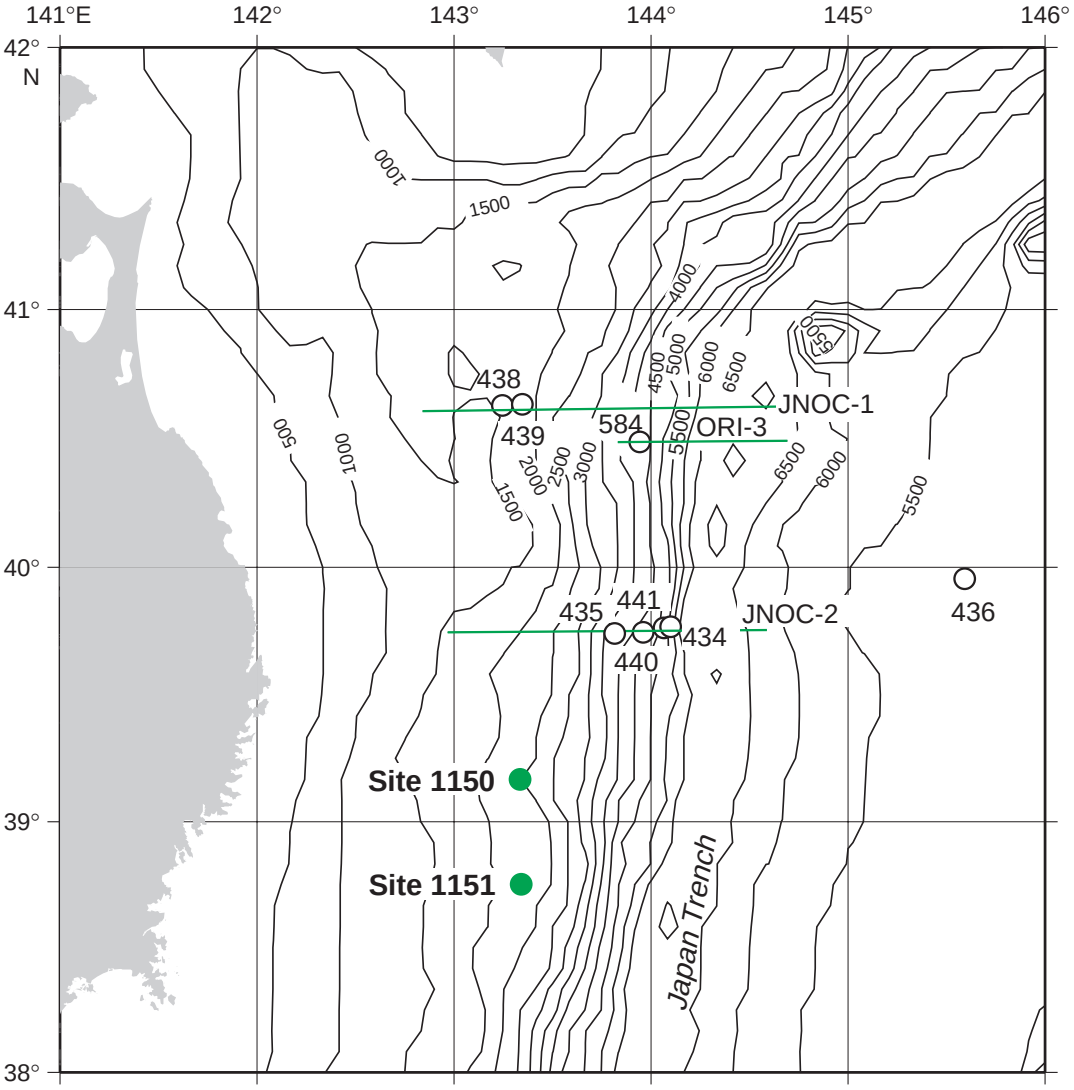

Figure F5. Frequency of ash patches averaged over 2 m.y. from Sites 1150 and 1151, indicating volcanic activity.

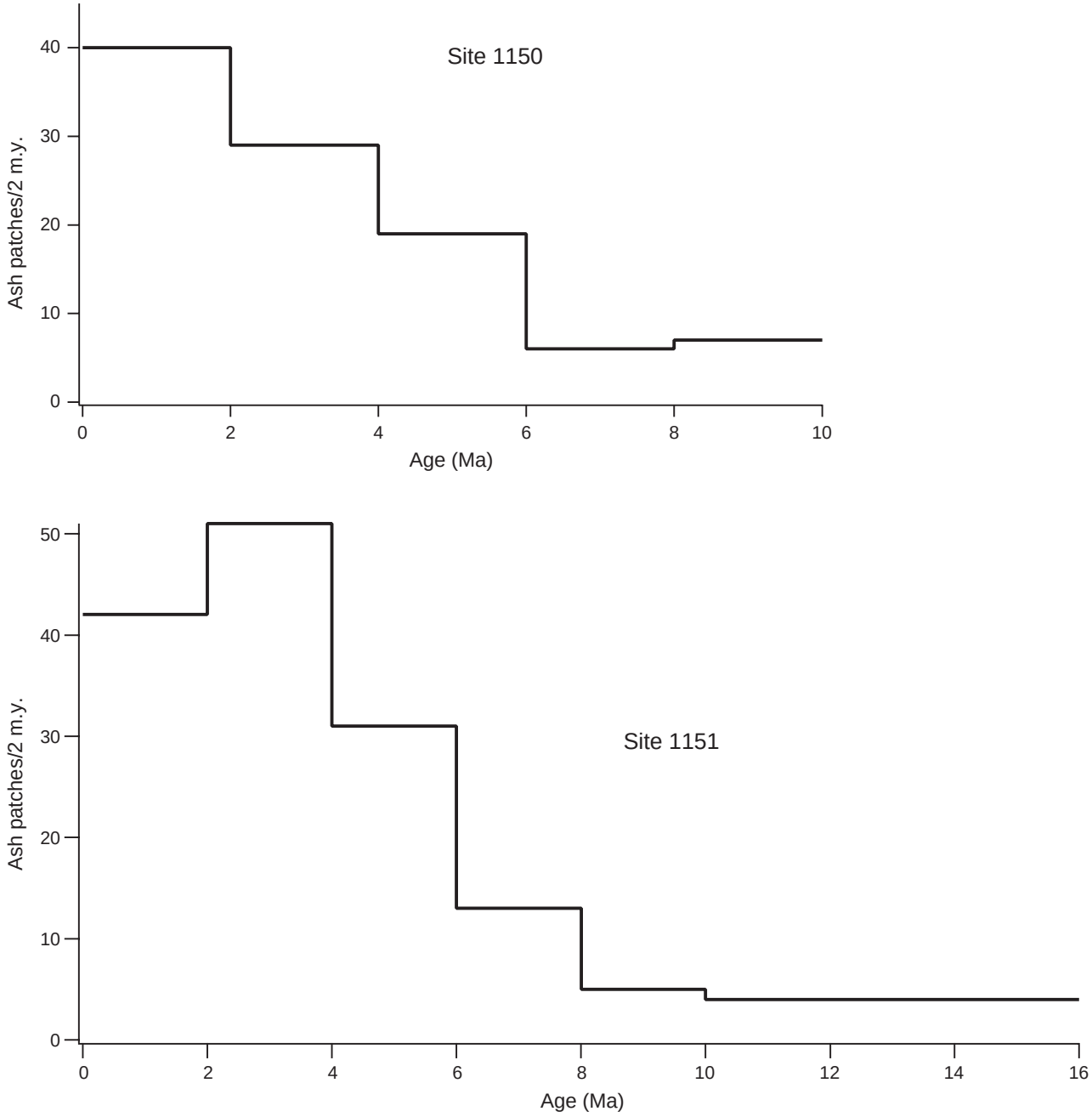

Figure F6. Sedimentation rates from cored samples in the forearc sites. Rates are given in meters per million years obtained for every 1-m.y. period. Correction for compaction is not significant but is included.

Period (Ma)	Site 1150 (m/m.y.)	Site 1151 (m/m.y.)
0-1	122	103
1-2	67	29
2-3	288	62
3-4	130	74
4-5	587	330
5-6	198	169
6-7	80	270
7-8	155	36
8-9	68	123
9-10	106	67
10-11		55
11-12		37
12-13		22
13-14		8
14-15		63
15-16		63

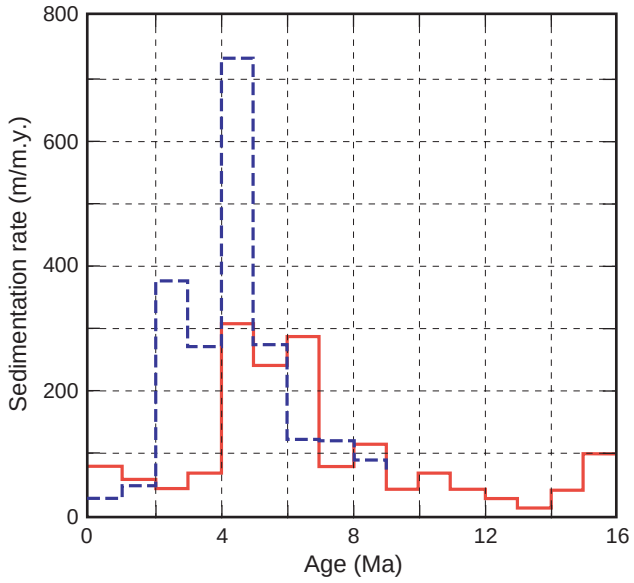

Figure F7. Geochemical signature of interstitial water from core samples (from Sacks, Suyehiro, Acton, et al., 2000).

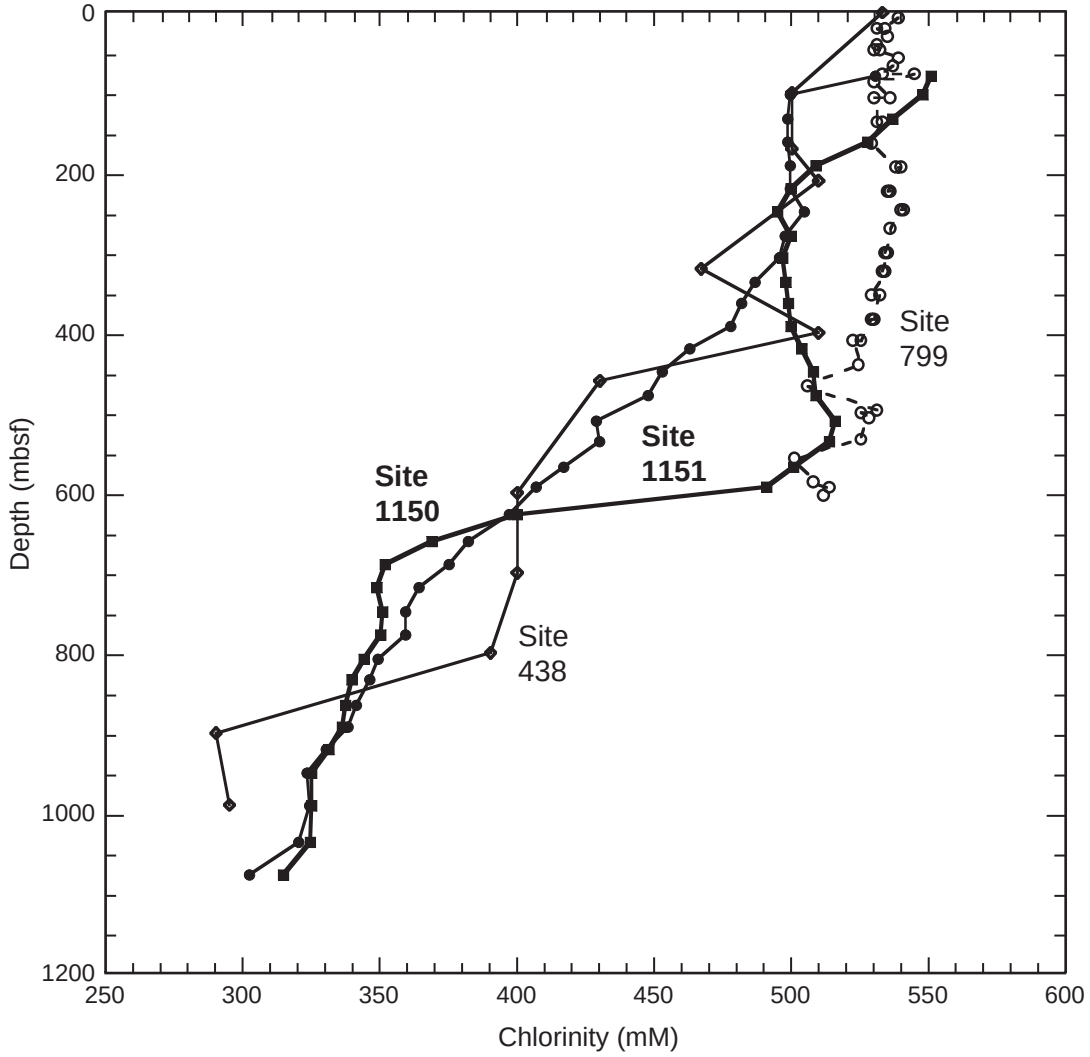

Figure F8. Stress field change since 22 Ma of the Japan arc and backarc (from Sato and Amano, 1991; Uyeda, 1982, Sugi et al., 1983; Jolivet and Tamaki, 1992).

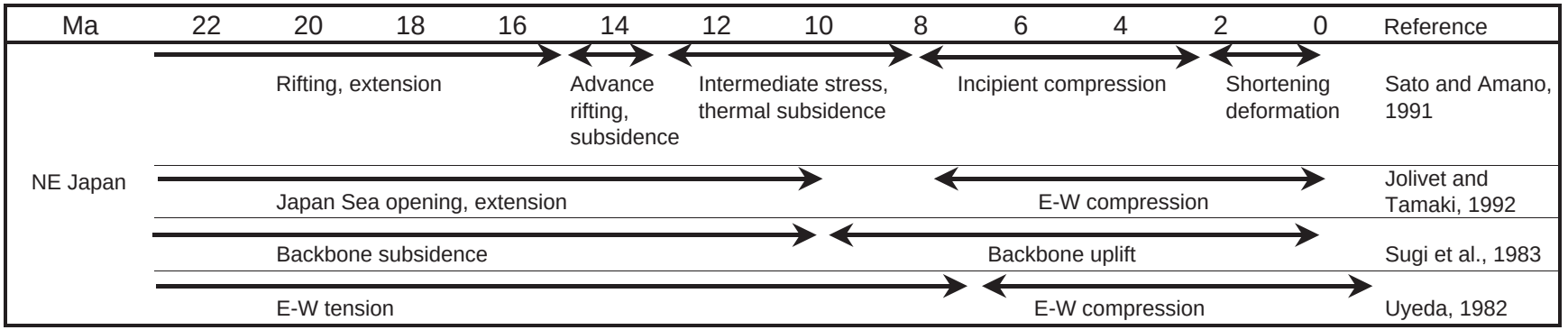

Figure F9. Migration of the volcanic front (VF) from Ohguchi et al. (1989). Offshore position of the VF at ~20 Ma is estimated from the drilled evidence (Moore and Fujioka, 1980). Two curves are drawn for 16/14 Ma depending on inclusion of the Hachinohe-oki volcanic rock. There are also two estimates for 12 Ma, but these are not relevant in this paper.

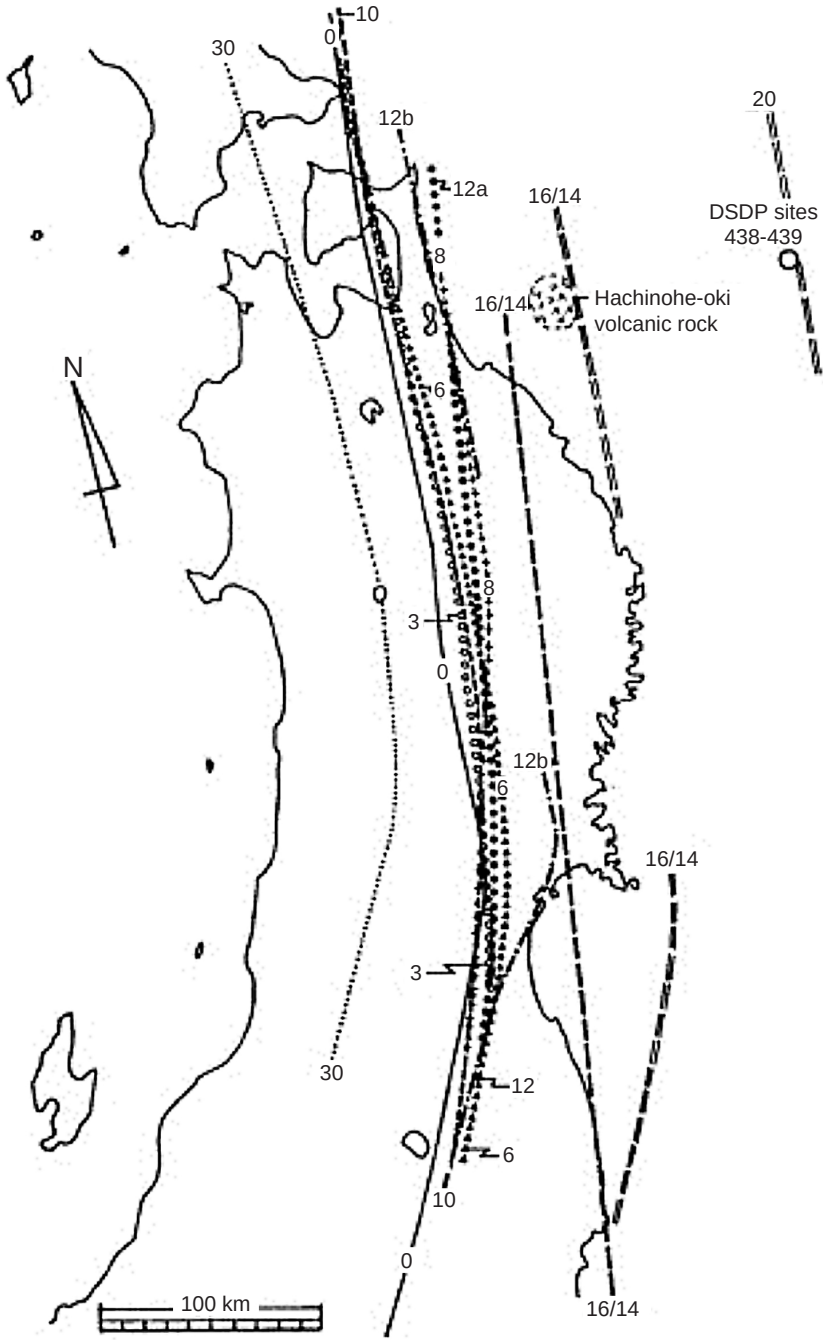

Figure F10. Change in plate geometry over time. **A.** Effect of subduction erosion (from von Huene and Lallemand, 1990). **B.** Overall estimation of plate geometry relative to the Asian continent (locations of the VF [volcanic front] relative to arbitrary origin on the Asian continent are given at bottom right) assuming constant (~100 km) depth to the subducting plate boundary from VF and past VF locations (Fig. F9, p. 22). The VF and TA (trench axis) for each period are shown with their age. Plate geometry at 25 Ma is not certain, and two probable geometries are shown.

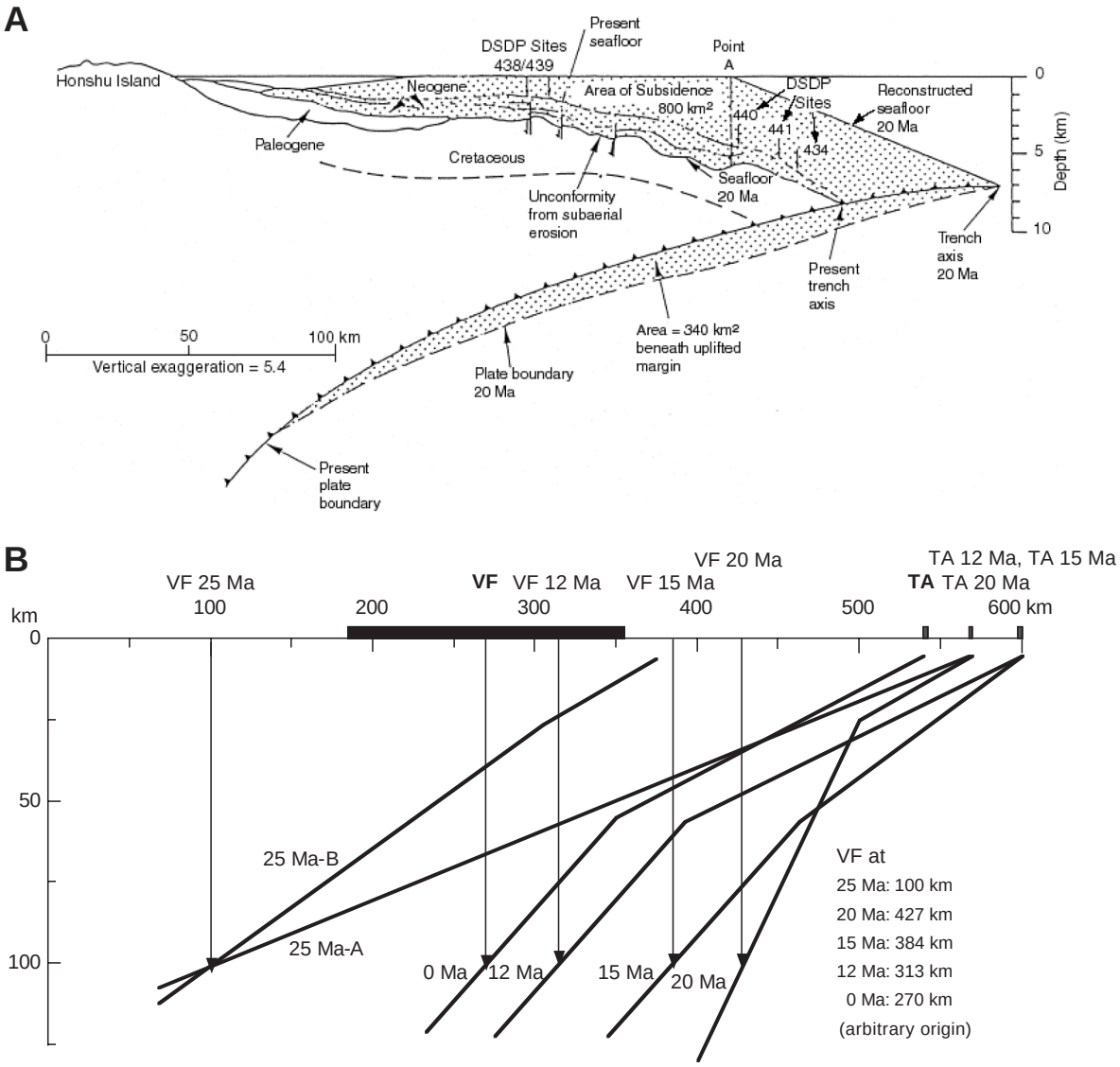

Figure F11. Development of stiffened mantle wedge. Cooling of mantle material to the surface and to the slab in the narrow wedge causes higher viscosity so that the flow will lag. Eventually the nose becomes essentially static (after Kincaid and Sacks, 1997).

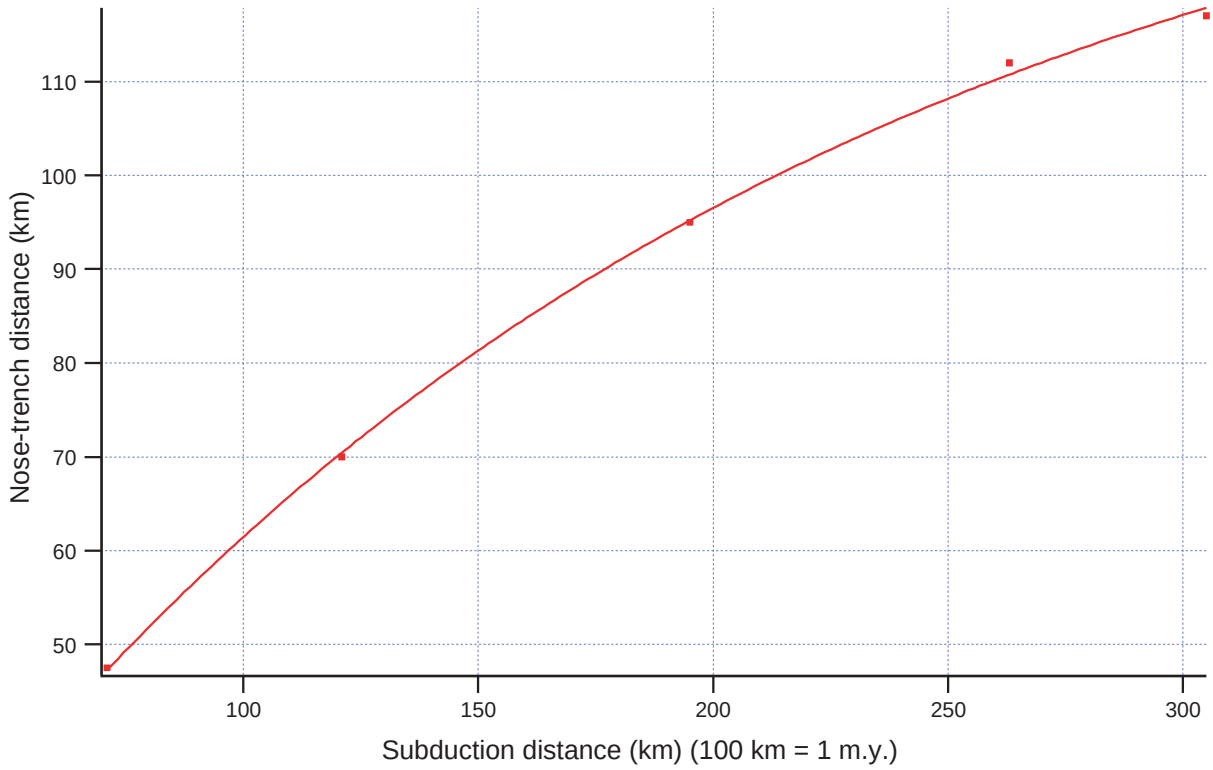

Figure F12. Estimated plate coupling length change since 20 Ma. The two horizontal lines represent the surface and Moho. Numbers are depths in kilometers. The thickened zone indicates a coupled zone. **A.** 20 Ma: steep subduction resembling the present subduction in the Marianas. **B.** 20–14 Ma: dip angle decreases. **C.** 10–6 Ma: subduction erosion proceeds. **D.** 6–4 Ma: stiffening of mantle wedge nose proceeds. **E.** 4–0 Ma: downdip end of coupled zone becomes shallower as hydration proceeds.

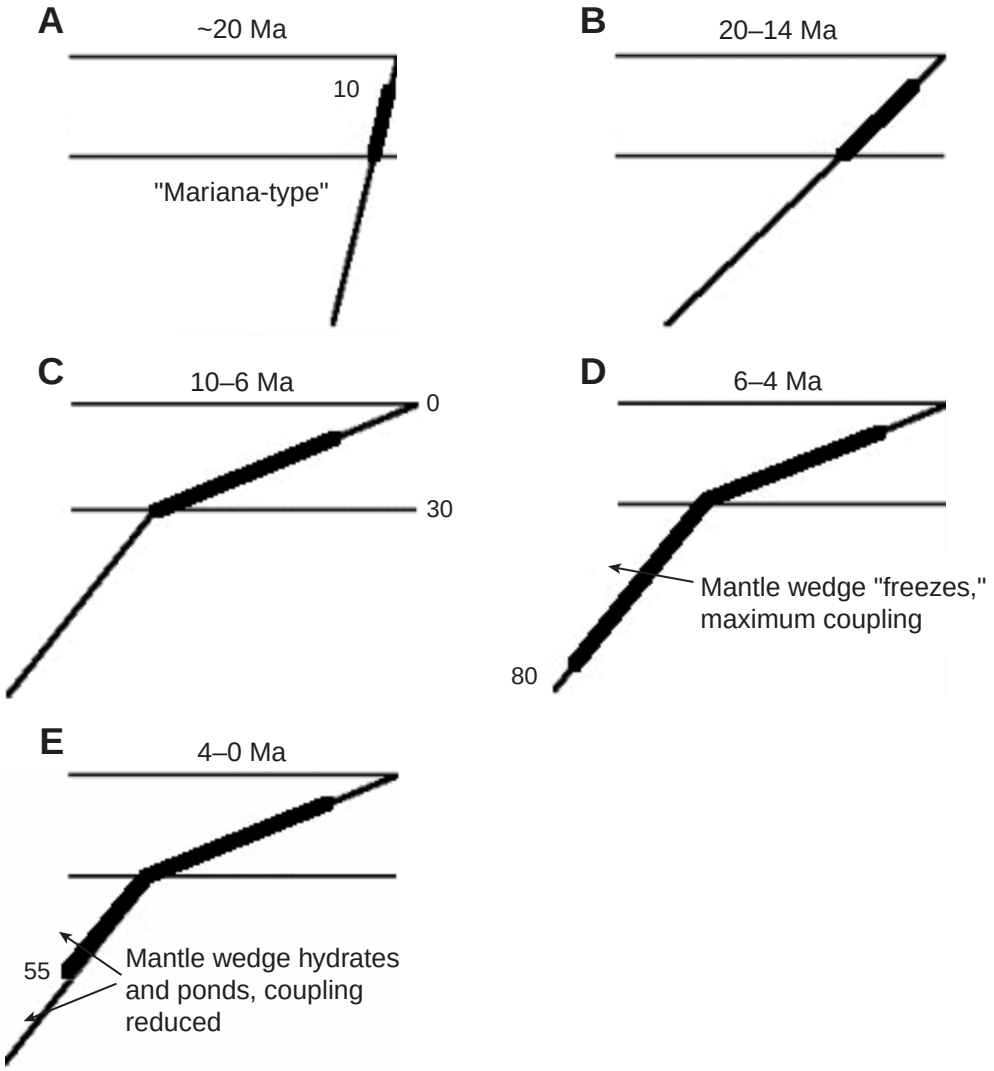

Figure F13. Summary diagram showing relation of sedimentation rate and volcanic flux to age for Sites 1150 and 1151. Blue = corrected sedimentation rate, green = number of ash patches per 2 m.y., red = model sedimentation rate from the square of the coupling length.

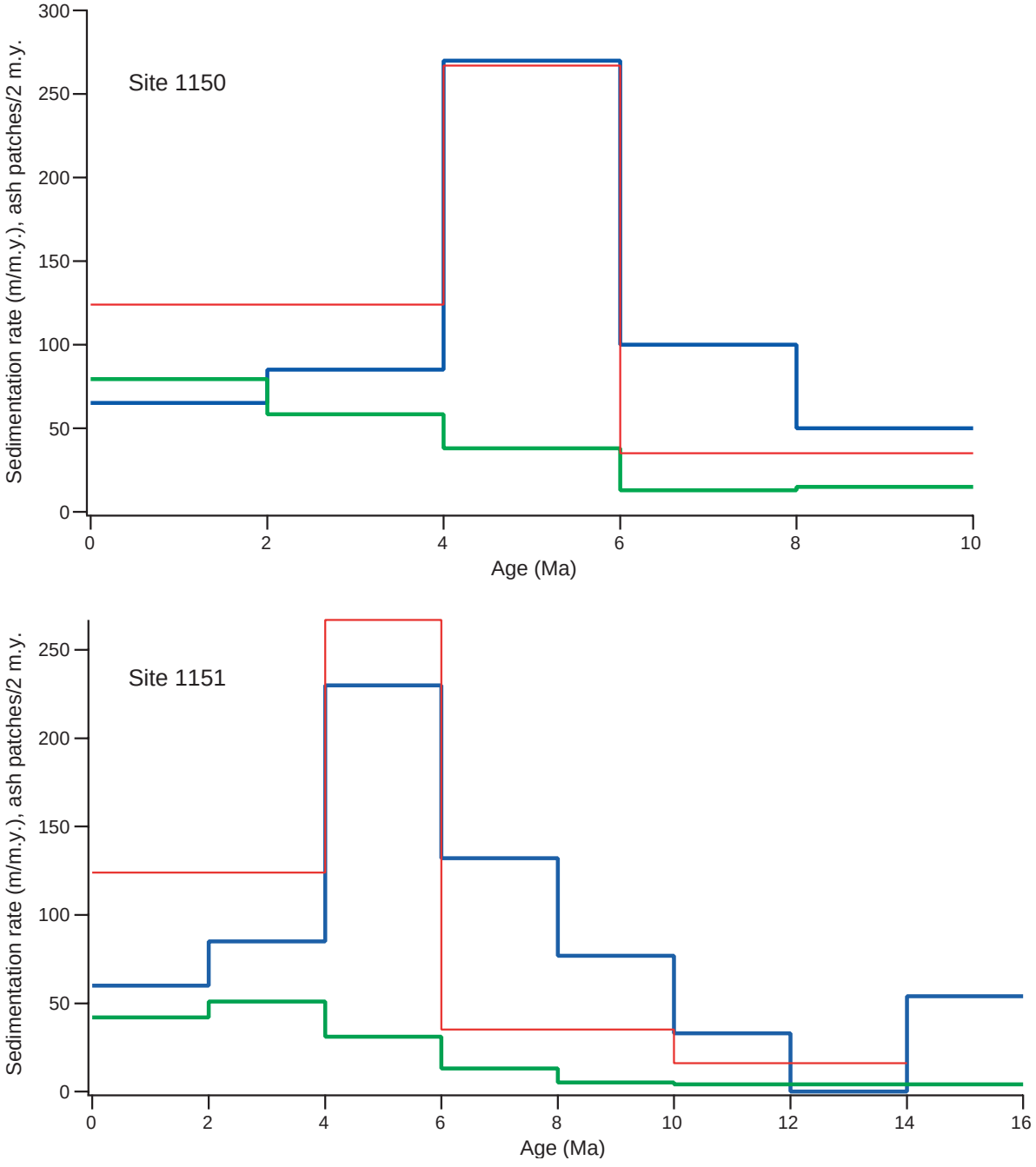

CHAPTER NOTE*

N1. Araki, E., Shinohara, M., Sacks, S., Linde, A, Kanazawa, T., and Suyehiro, K., submitted. Improvement of seismic observation in the ocean by use of ocean boreholes. *Bull. Seismol. Soc. Am.*

*Dates reflect file corrections or revisions.